

Chalcogen-height dependent magnetic interactions and magnetic order switching in $\text{FeSe}_x\text{Te}_{1-x}$

Chang-Youn Moon and Hyoung Joon Choi*

Department of Physics and IPAP, Yonsei University, Seoul 120-749, Korea

(Dated: November 10, 2018)

Magnetic properties of iron chalcogenide superconducting materials are investigated using density functional calculations. We find the stability of magnetic phases is very sensitive to the height of chalcogen species from the Fe plane: while FeTe with optimized Te height has the double-stripe-type $(\pi, 0)$ magnetic ordering, the single-stripe-type (π, π) ordering becomes the ground state phase when Te height is lowered below a critical value by, e.g., Se doping. This behavior is understood by opposite Te-height dependences of the superexchange interaction and a longer-range magnetic interaction mediated by itinerant electrons. We also demonstrate a linear temperature dependence of the macroscopic magnetic susceptibility in the single-stripe phase in contrast to a constant behavior in the double-stripe phase. Our findings provide a comprehensive and unified view to understand the magnetism in $\text{FeSe}_x\text{Te}_{1-x}$ and iron pnictide superconductors.

PACS numbers: 71.15.Mb, 71.20.-b, 75.25.+z

In a short period of time since the recent discoveries [1, 2, 3], the research of iron-based superconductors (SC) has been extended to a large variety of materials. Among them, iron chalcogenides $\text{FeSe}_x\text{Te}_{1-x}$ are unique with their structural simplicity that they are composed of only iron-based layers while maintaining the same nominal Fe^{2+} charge state as the iron pnictides. Unlike most of iron SCs which have to be substantially doped to suppress the inherent antiferromagnetism (AFM) and develop the superconductivity, undoped FeSe is not magnetically ordered, superconducting with $T_c \sim 9\text{K}$ [4, 5], while undoped FeTe is not superconducting but magnetically ordered. Very uniquely, FeTe has an AFM ordering pattern, so called “double stripe” with $(\pi, 0)$ ordering vector [6, 7], while all other iron-based superconducting materials exhibit “single stripe” type ordering pattern with the (π, π) ordering vector.

Nature of magnetism in iron SCs has been a controversial issue between Fermi surface (FS) nesting and local spin moment interactions. Several recent works suggest unified pictures based on local moment interactions including some role of itinerant electrons but not in the way as in FS nesting scenario [8, 9, 10, 11, 12, 13, 14, 15, 16]. Since FeTe has the (π, π) FS nesting similarly to other iron SCs [17], the observed $(\pi, 0)$ magnetic ordering in FeTe may indicate irrelevance of FS nesting mechanism at least for FeTe [7]. A recent first-principles study [18] suggests the emergence of $(\pi, 0)$ FS nesting assuming substantial electron doping by excess Fe, however, this doping effect was not observed in an angle-resolved photoemission experiment [19].

The magnetic stability of $(\pi, 0)$ ordering over (π, π) in FeTe can be effectively described by the nearest, second nearest, and third nearest neighbor exchange parameters, J_1 , J_2 , and J_3 , respectively, with the condition $J_3 > J_2/2$ [7]. However, what makes such a condition hold uniquely for FeTe, neither FeSe nor iron pnictides, is not uncov-

ered. Furthermore, the absence of linear temperature (T) dependence of magnetic susceptibility in FeTe [6, 19], in contrast to other iron SCs, is yet to be understood.

In this paper, we perform the first-principles calculations to investigate magnetic properties of iron chalcogenides. We find that Te height from the Fe plane is a key factor which determines AFM ordering patterns in FeTe, so that the ground state magnetic ordering changes from the $(\pi, 0)$ with the optimized Te height to the (π, π) patterns when Te height is lowered. We observe the same effect with FeSe, concluding that it is not chalcogen species but chalcogen position that determines the magnetic ordering in $\text{FeSe}_x\text{Te}_{1-x}$, and that this feature originates from different chalcogen-height dependences of J_1 , J_2 , and J_3 . Our calculated macroscopic magnetic susceptibilities (χ_M) for (π, π) and $(\pi, 0)$ AFM orderings show linear and constant T dependences, respectively, suggesting a clue to understand the puzzling T dependences of χ_M measured in iron SCs. Our results, altogether, provide a comprehensive view on the magnetism in $\text{FeSe}_x\text{Te}_{1-x}$ and iron pnictide SCs.

Our first-principles calculations are based on the density-functional theory with the generalized gradient approximation [20] and the *ab-initio* norm-conserving pseudopotentials as implemented in SIESTA code [21]. Semicore pseudopotentials are used for Fe, and electronic wave functions are expanded with localized pseudoatomic orbitals (double zeta polarization basis set), with the cut-off energy of 500 Ry for real space mesh. Brillouin zone integration is performed with $6 \times 6 \times 6$ k-point grid using a $2a \times 2a \times c$ supercell which contains 8 Fe and 8 Te atoms, and is commensurate with both the double- and single-stripes AFM ordering patterns.

The atomic structure of FeTe is shown in Fig. 1(a). Fe atoms form a plane and Te atoms are bonded to Fe atoms above and below the Fe plane, and the distance of a Te atom from the Fe plane is defined as the Te height

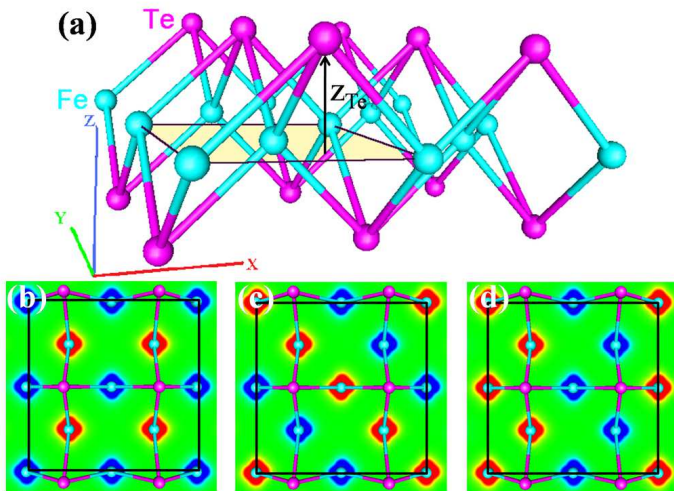


FIG. 1: (Color online). (a) Atomic structure of FeTe where z_{Te} is defined with respect to the Fe plane marked by a shaded square. Spin densities of (b) AFM1, (c) AFM2, and (d) AFM3 phases are displayed on the $z = 0$ plane, and the supercell is denoted by a black square in each figure.

(z_{Te}) as shown in the figure. Structural optimization is performed with the unit-cell lattice constants fixed to the experimental high-temperature tetragonal structure measured at 80 K, $a = c = 3.812 \text{ \AA}$ and $c = 6.252 \text{ \AA}$ [6], although the low temperature AFM phase is associated with a monoclinic structure. This is for simplicity in defining z_{Te} and easy comparison with FeSe case. We have checked that this simplification does not alter our main conclusion. We consider ferromagnetic (FM) phase and three different AFM phases to study the magnetic properties: ‘checkerboard’ (Fig. 1(b)), ‘single stripe’ (Fig. 1(c)), and ‘double stripe’ (Fig. 1(d)) type orderings, which hereafter are referred to as AFM1, AFM2, and AFM3, respectively.

To investigate effects of chalcogen height on magnetic orderings, we calculate energetic stabilities of magnetic phases as a function of z_{Te} . Starting from the optimized z_{Te} of 1.81 \AA , the total energies of FM, AFM1, AFM2, and AFM3 phases are calculated with decreasing z_{Te} as shown in Fig. 2(a). At optimized z_{Te} , AFM3 is most stable in agreement with the experiment and the previous calculation [6, 7], and AFM2 is slightly higher in energy by 32 meV per Fe. Interestingly, FM phase is found to be more stable than AFM1 phase in contrast to our previous experience on iron pnictides that FM phase relaxes to the non-magnetic (NM) state without a constraint on the magnetic moment and has higher energies than AFM phases even with a fixed spin moment (FSM) calculation. When z_{Te} is decreased to 1.75 \AA , AFM3 is still more stable than AFM2 but the energy difference reduces. After z_{Te} is further decreased approximately below 1.71 \AA (see the vertical arrow in Fig. 2(a)), finally AFM2 phase turns more stable than AFM3 phase, and

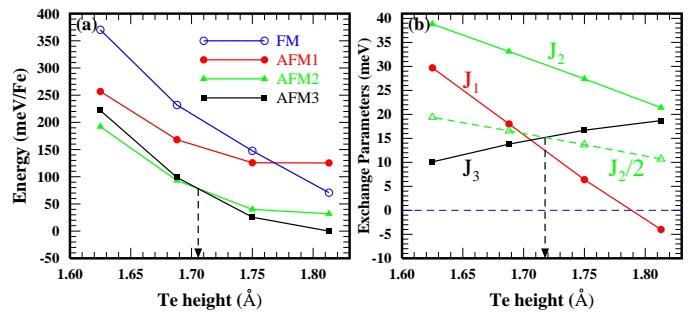


FIG. 2: (Color online). (a) Total energy versus z_{Te} calculated for FM, AFM1, AFM2, and AFM3 phases. (b) Exchange parameters J 's are shown as functions of z_{Te} which are evaluated with fixed Fe magnetic moment of $2.95 \mu_B$. Vertical arrows denote the critical z_{Te} 's where AFM2-AFM3 switch takes place which are slightly different in (a) and (b) due to different treatment of local magnetic moments (see text).

the relative stability of AFM2 over AFM3 phases is even enlarged as z_{Te} is decreased further to 1.63 \AA , towards our optimized Se height 1.55 \AA of FeSe. The Fe magnetic moment is decreasing along with z_{Te} , and the averaged values over the three AFM phases for each z_{Te} are 2.94 , 2.84 , 2.72 , and $2.58 \mu_B$ for $z_{Te} = 1.81$, 1.75 , 1.69 , and 1.63 \AA , respectively. Except for the $z_{Te} = 1.81 \text{ \AA}$ case, we need to perform the FSM calculation to obtain the FM phase, in which the Fe moment is fixed to the average value of the three AFM phases with the same z_{Te} .

Since AFM3 ordering in FeTe is apparently incompatible with the FS nesting scenario, we consider Heisenberg type local moment interactions, and estimate the three exchange parameters J_1 , J_2 , and J_3 , as functions of z_{Te} , from the calculated total energies of each magnetic phase and z_{Te} . Since J 's depend on the magnitude of the magnetic moment in general [22], we perform the FSM calculations, with the Fe spin moment being fixed to $2.95 \mu_B$ (the value for AFM3 at $z_{Te} = 1.81 \text{ \AA}$), for all the magnetic phases and z_{Te} . The result is shown in Fig. 2(b). At optimized $z_{Te} = 1.81 \text{ \AA}$, J_2 is largest, while J_1 is estimated to be negative as the FM phase is more stable than AFM1 phase at this z_{Te} , and J_3 is almost comparable with J_2 . As z_{Te} decreases, we see a clear tendency that J_1 and J_2 increase while J_3 decreases. Around $z_{Te} = 1.72 \text{ \AA}$, $J_2/2$ starts to exceed J_3 which reflects that AFM2 phase becomes more stable than AFM3 from this point on. We should note that this critical value of z_{Te} is slightly different from the one in Fig. 2(a) where the magnetic moments are unrestricted, while they are fixed in the estimation of J 's as mentioned above.

In a word, the switch of ground state magnetic phase between AFM2 and AFM3 with varying z_{Te} is due to opposite z_{Te} dependence between J_2 (along with J_1) and J_3 . The behavior of J_1 and J_2 can be understood relatively easily if we recall their superexchange nature [22]. As Te atom gets close to the Fe plane, Fe-Te-Fe angle

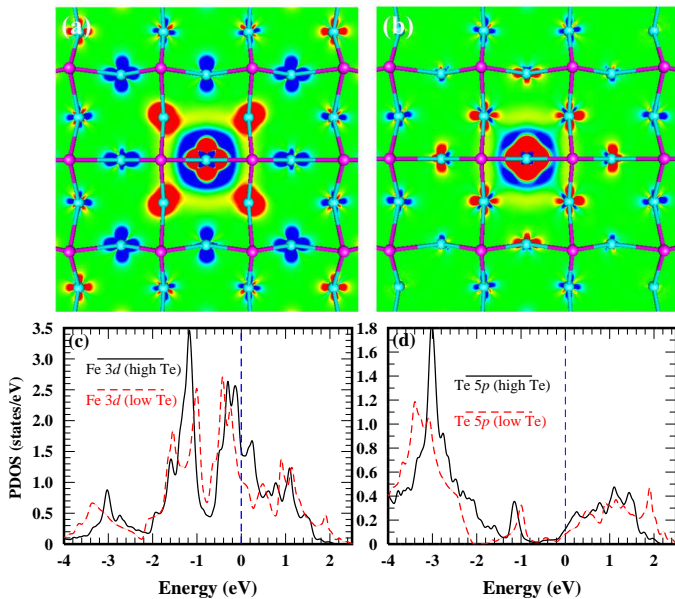


FIG. 3: (Color online). Magnetic susceptibility $\chi_s(r, r' = 0; \omega = 0)$ of the NM phase is shown for (a) $z_{Te} = 1.81$ and (b) $z_{Te} = 1.63$ Å. Delta-like magnetic field is applied at the center of the figure. PDOS in the NM phase is displayed for (c) Fe 3d and (d) Te 5p states.

approaches 180° which maximizes the overlap between Te 5p and Fe 3d orbital lobes, and the superexchange interaction should get stronger. As for J_3 , a longer-range interaction is needed where isolated local spin moments can be coupled via itinerant electrons around the Fermi energy (E_F), such as so-called RKKY interaction.

To understand z_{Te} dependence of J_3 , we consider how a localized magnetic perturbation polarizes the surrounding initially spin-unpolarized electron cloud. We apply a delta-like magnetic field on a Fe atom of the *FeTe* system in the NM phase, by adding a potential difference between spin up and down electrons at the center of the Fe atom, and obtaining self-consistent electron spin density in response to this external field, as displayed in Figs. 3(a) and (b). By definition, this plot corresponds to $\chi_s(r, r' = 0; \omega = 0)$ when the delta field is applied to the origin. Here we use $2 \times 2 \times 1$ enlarged supercell of our original supercell shown in Fig. 1 to reduce the effect of other external fields from the periodic images of the supercell. When Te is at the optimized height 1.81 Å (Fig. 3(a)), the electron cloud is strongly spin-polarized by the delta field and show an alternating pattern, with a slow decay rate with distance from the origin. In the meanwhile, when z_{Te} is lowered down to 1.63 Å in Fig. 3(b), the spin polarization decays much more rapidly away from the origin. Hence, $\chi_s(r, r' = 0; \omega = 0)$ for the NM phase becomes much more short-ranged with smaller z_{Te} , consistently with the fact J_3 decreases with decreasing z_{Te} .

The z_{Te} dependence of χ_s can be understood by analyzing the change in the electronic structure along with

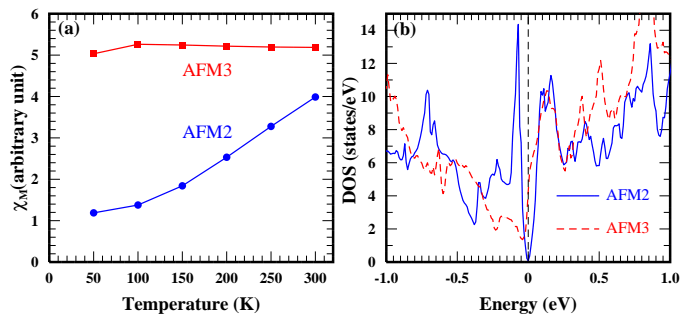


FIG. 4: (Color online). (a) Macroscopic magnetic susceptibility χ_M versus electron temperature is shown for two AFM orderings. (b) DOS of FeTe for AFM2 and AFM3 phases.

varying z_{Te} . Figure 3(c) represents the projected density of states (PDOS) on Fe 3d, where two peaks around -3 eV and E_F have t_{2g} character. When Te is lowered, the t_{2g} states couple to Te 5p states more strongly so that the corresponding peaks around -3 eV in Fig. 3(c) and (d) move down to the higher binding energy, gaining more Fe t_{2g} weight and losing Te 5p weight with an effective charge transfer from Te to Fe. Then the density of states (DOS) at E_F is greatly reduced due to the Fe t_{2g} weight transfer to the states around -3 eV and overall charge transfer to Fe states. This in turn results in generally reduced magnetic susceptibility χ_s , since it depends on the number of states around E_F (which correspond to ‘itinerant electrons’). The higher DOS at E_F for high z_{Te} also explains the stabilization of the FM phase at $z_{Te} = 1.81$ Å shown in Fig. 2, according to the Stoner criterion.

The Curie-Weiss-like behavior, i.e., the $1/T$ dependence of magnetic susceptibility is a peculiar feature measured in FeTe [6, 19] which undoubtedly shows the local nature of magnetism, while other iron-base SCs show linear- T dependence. Motivated by the fact the ground-state magnetic phase is AFM3 for FeTe and AFM2 for other iron SCs, we evaluate the macroscopic magnetic susceptibility χ_M for different magnetic orderings, as a function of electron temperature by applying a uniform magnetic field and obtaining self-consistent electron spin density. The result is shown in Fig. 4(a). The difference is obvious: χ_M depends linearly on T for AFM2 while it is almost constant for the AFM3 phase. This difference results from the dramatic difference in DOS at E_F , shown in Fig. 4(b). AFM2 phase has a large dip in DOS at E_F because of the band-repulsion between electron and hole bands which are separated by the $q = (\pi, \pi)$ vector in the Brillouin zone of the NM phase [16], while DOS at E_F is large in AFM3 phase because the perturbing potential by the magnetic ordering has only $q = (\pi, 0)$ component which cannot couple the electron and hole FSs. Since the susceptibility is larger when there is large number of states around E_F , the overall value of χ_M is smaller for AFM2 phase. However, as the electron temperature

increases with the Fermi-Dirac distribution, more states become available to participate in the magnetic response and χ_M rises.

For χ_M in high-temperature paramagnetic phase, we consider canonical ensemble of local spin moments, in which the probability of each configuration is given by the Boltzmann factor associated mainly with the Heisenberg Hamiltonian. When a uniform magnetic field is applied, χ_M has $1/T$ -like dependence if the spin moments are frozen in each configuration. With itinerant electrons, χ_M also has contribution from field-induced spin-density change in each configuration averaged by the Boltzmann factor, which is dominated by the ground state and low-energy configurations possibly composed of disordered domains of the ground-state AFM phase [23]. Then, the spin-density change in the ground-state AFM will contribute significantly to χ_M in the paramagnetic phase. Thus we suggest χ_M in the paramagnetic phase has a linear- T component for lower chalcogen height, while the component is absent for higher chalcogen height.

We also have checked that the ground states in FeSe and LaFeAsO, which are AFM2 with optimized atomic positions, change to AFM3 when Se or As height is increased. This implies the magnetism in FeTe in fact is not qualitatively different from that of other iron-based SCs, and the peculiar $(\pi, 0)$ ordering pattern is just a specific realization among many possible magnetic orderings determined by the relative strength of local-moment exchange interactions J 's, which can be controlled continuously by varying the chalcogen (and pnictogen) height, for example, by alloying such as $\text{FeSe}_x\text{Te}_{1-x}$. Although FeSe and other alloys with FeTe are not experimentally reported to exhibit any magnetically ordered phase possibly due to the off-stoichiometry etc., our results suggest that AFM2 is the lowest-energy configuration in the canonical ensemble for paramagnetic $\text{FeSe}_x\text{Te}_{1-x}$ with x over a critical value. This possibly results in the linear- T dependence of χ_M as demonstrated above. However, when Se concentration is not enough, the chalcogen height is so high that AFM3 is the lowest-energy configuration, and the Curie-Weiss-like $1/T$ dependence of χ_M [6, 19], ordinary for the local moment magnetism, is observed in the paramagnetic phase.

Increasing Se in $\text{FeSe}_x\text{Te}_{1-x}$ is reported to suppress $(\pi + \delta, 0)$ spin fluctuation and enhance (π, π) fluctuation with the superconductivity [24]. Our result shows that this might be related to the continuous change of the relative energy between AFM3 and AFM2 orderings with increasing x . When x is small and chalcogen height is large, the AFM3 state and $(\pi, 0)$ spin fluctuation has greater probability in the canonical ensemble for the paramagnetic phase, weakening the interaction between electron and hole FSs separated by $q = (\pi, \pi)$. As x increases over the critical value, the AFM2 state and (π, π) spin fluctuation start to take over, which coincides with the superconductivity observed in $\text{FeSe}_x\text{Te}_{1-x}$. Therefore, our result

shows that the superconductivity in iron chalcogenides may be related to (π, π) spin ordering and fluctuations as likely as in iron pnictides. Our findings further suggest that the superconducting state might be realized in FeTe by controlling the Te height by, such as, applying a biaxial strain.

In conclusion, we show that the unique magnetic ordering in FeTe is due to the relatively high chalcogen height compared with FeSe as the underlying magnetic interactions depend on the chalcogen height in different ways. This behavior is found to apply for other iron chalcogenide and iron pnictides, hence the magnetism in iron-based SCs including FeTe can be understood with a same unified mechanism. Temperature dependence of magnetic susceptibility evaluated for the AFM2 and AFM3 phases sheds light on the puzzling experimental results observed for $\text{FeSe}_x\text{Te}_{1-x}$.

This work was supported by NRF of Korea (Grant No. 2009-0081204) and KISTI Supercomputing Center (Project No. KSC-2008-S02-0004).

* Email: h.j.choi@yonsei.ac.kr

- [1] Y. Kamihara *et al.*, *J. Am. Chem. Soc.* **128**, 10012, (2006).
- [2] Y. Kamihara, T. Watanabe, M. Hirano, and H. Hosono, *J. Am. Chem. Soc.* **130**, 3296, (2008).
- [3] H. Takahashi *et al.*, *Nature (London)* **453**, 376 (2008).
- [4] F. C. Hsu *et al.*, *Proc. Natl. Acad. Sci. U.S.A.* **105**, 14262 (2008).
- [5] T. M. McQueen *et al.*, *Phys. Rev. B* **79**, 014522 (2009).
- [6] S. Li *et al.*, *Phys. Rev. B* **79**, 054503 (2009).
- [7] F. Ma, *Phys. et al.*, *Phys. Rev. Lett.* **102**, 177003 (2009).
- [8] J. Wu, P. Phillips, and A. H. Castro Neto, *Phys. Rev. Lett.* **101**, 126401 (2008).
- [9] J. Wu and P. Phillips, arXiv:0901.3538v1.
- [10] S.-P. Kou, T. Li, and Z.-Y. Weng, arXiv:0811.4111v3.
- [11] G. D. Samolyuk and V. P. Antropov, *Phys. Rev. B* **79**, 052505 (2009).
- [12] J. Zhang, R. Sknepnek, R. M. Fernandes, and J. Schmalian, *Phys. Rev. B* **79**, 220502(R) (2009).
- [13] E. Manousakis, *Phys. Rev. B* **79**, 220509(R) (2009).
- [14] M. D. Johannes and I. I. Mazin, *Phys. Rev. B* **79**, 220510(R) (2009).
- [15] C.-Y. Moon, S. Y. Park, and H. J. Choi, *Phys. Rev. B* **78**, 212507 (2008).
- [16] C.-Y. Moon, S. Y. Park, and H. J. Choi, *Phys. Rev. B* **80**, 054522 (2009).
- [17] A. Subedi, L. Zhang, D. J. Singh, and M.-H. Du, *Phys. Rev. B* **78**, 134514 (2008).
- [18] M. J. Han and S. Y. Savrasov, *Phys. Rev. Lett.* **103**, 067001 (2009).
- [19] Y. Xia *et al.*, *Phys. Rev. Lett.* **103**, 037002 (2009).
- [20] J. P. Perdew, K. Burke, and M. Ernzerhof, *Phys. Rev. Lett.* **77**, 3865 (1996).
- [21] D. Sanchez-Portal, P. Ordejon, E. Artacho, and J. M. Soler, *Int. J. Quantum Chem.* **65**, 453 (1997).
- [22] T. Yildirim, *Phys. Rev. Lett.* **101**, 057010 (2008).
- [23] I. I. Mazin and M. D. Johannes, *Nat. Phys.* **5**, 141 (2009).

[24] K. Nakayama *et al.*, arXiv:0907.0763v1 (2009).